Nature. Author manuscript; available in PMC 2021 August 23.

Published in final edited form as:
Nature. 2014 January 09; 505(7482): 180–5. doi:10.1038/nature12879.

Patterning and growth control by membrane-tethered Wingless

Cyrille Alexandre[+], **Alberto Baena-Lopez**[+], **Jean-Paul Vincent**
MRC National Institute for Medical Research, The Ridgeway, Mill Hill, London NW7 1AA, United Kingdom

Abstract

Wnts are evolutionarily conserved secreted signaling proteins that, in various developmental contexts, spread from their site of synthesis to form a gradient and activate target gene expression at a distance. However, the requirement for Wnts to spread has never been directly tested. Here we used genome engineering to replace the endogenous *wingless* gene, which encodes the main *Drosophila* Wnt, with one that expresses a membrane-tethered form of the protein. Surprisingly, the resulting flies were viable and produced normally patterned appendages of nearly the right size, albeit with a delay. We show that, in the prospective wing, prolonged *wingless* transcription followed by memory of earlier signaling allow persistent expression of relevant target genes, thus explaining why Wingless release is dispensable. We suggest that patterning and growth can proceed without an instructive Wingless gradient, even though the spread of Wingless likely increases the rate of proliferation.

Introduction

Wnts are secreted signaling proteins [1,2] that have been suggested to act at a distance to control patterning and growth during development [3]. Long range Wnt activity has been most extensively studied in wing imaginal discs of Drosophila [4–6]. These epithelial pockets, set aside in the embryo, grow from 50 to ~50,000 cells during larval stages to give rise to fully patterned wings during pupariation [7–9]. During early larval life, Wingless, the main Drosophila Wnt, is initially expressed throughout the prospective wing field to establish wing primordium [10–14] At subsequent stages, Wingless is produced in a narrow stripe of cells at the dorso-ventral (D-V) boundary. It is thought that from there, it spreads throughout the prospective wing blade and activate target gene expression in a concentration-dependent manner [4–6]. A common view is that, near the D-V boundary, high signaling activity activates *senseless* expression, which contributes to wing margin fates [15–17] while further away, in the prospective wing blade (up to 50 cell diameters), low level of signaling stimulates the expression of more sensitive target genes like *vestigial, distalless* and *frizzled3* [4,5,18,19] and

Correspondence to: Jean-Paul Vincent.

Correspondence and requests for materials should be addressed to JPV (jvincen@nimr.mrc.ac.uk).
[+]Equivalent first authors

Author Contributions
All the experiments were performed jointly by LAB and CA. The three authors contributed equally to the conception of the work, the interpretation of results, and manuscript preparation.

Author Information
The authors declare no competing financial interests.

Europe PMC Funders Author Manuscripts

promotes growth [20,21]. Although the importance of graded Wingless signaling has been disputed [21], it is generally accepted that Wingless needs to spread over the whole wing field for patterning and growth. To test this assumption directly, we sought to modify the *wingless* locus so that membrane-tethered Wingless would be expressed at physiological level in the absence of the wild type form.

Patterning and growth by membrane-tethered Wingless

A fusion protein comprising the type 2 transmembrane protein Neurotactin and Wingless (NRT-Wingless) has been previously shown in clonal overexpression assays to activate target genes only within expressing cells and in surrounding adjoining cells[4,22,23]. As a first step towards introducing a cDNA encoding NRT-Wingless into the *wingless* locus, we used an improved protocol for homologous recombination [24] to delete the wild type ATG-containing exon and replace it with a cassette that includes an *attP* recombination site, a *cherry* reporter, and other elements (Extended Data Figure 1a). As expected, in heterozygous *larvae,* Cherry was expressed in a pattern that broadly recapitulated that of endogenous *wingless* (Extended Data Figure 1b). Most extraneous genetic elements were then removed leaving only the *attP* site and a single *LoxP* site at the locus (Extended Data Figure 1a). The resulting allele behaved as a null and is therefore referred hereafter as *wg[KO]* (Extended Data Figure 1a). A wild type *wingless* cDNA was inserted into the *attP* site, along with mini-white as a genetic marker, and the resulting flies *(wg[KO; Wg])* were indistinguishable from wild type flies, confirming faithful expression of the reintegrated cDNA (Extended Data Figure 1d,f,g). Next, a cDNA encoding HA-tagged NRT-Wingless was introduced at the targeted locus, using either *mini-white* or *pax*-Cherry as a genetic marker, to generate *wg[KO; NRT-Wg]* (Extended Data Figure 1e; See Methods for details about genetic marker usage throughout this manuscript). Remarkably, when grown without crowding, homozygous animals that have NRT-Wingless as their sole source of Wingless were viable and had normally patterned appendages and other cuticular structures (Fig. 1a, b; Extended Data Figure 1f-o). The wings were slightly smaller than those of control siblings (10-12% surface area reduction; Extended Data Figure 1f-i). However, the arrangement of margin sensory bristles appeared normal (as shown at high magnification in Extended Data Figure 1j-l), an indication of appropriate *senseless* expression during imaginal development. Other target genes, *vestigial* (not shown), *distalless* (immunofluorescence) and *frizzled3* (from a reporter) were mildly affected, with their expression dropping off more sharply than in controls but without a noticeable consequence on adult wing patterning (Fig. 1b). Importantly, these reporters of Wingless signaling continued to be expressed in a broad domain straddling the D-V boundary (Fig. 1c-f).

Signaling by NRT-Wingless is juxtacrine

How could NRT-Wingless activate target genes seemingly at a long range? Staining of homozygous *wg[KO; NRT-Wg]* imaginal discs with anti-Wingless showed a restricted distribution by comparison to that in control discs although weak staining could be detected at the surface of cells located on either side of the main expression domain (Fig. 1g-h). To assess whether this could be due to protein perdurance or release (e.g. by cleavage or on exosomes), we devised a system for timed removal of the NRT-Wingless cDNA. A *wg[KO;*

FRT**.NRT-Wg.**FRT**]* allele was created and combined with *hedgehog-gal4, UAS-flp* and *tubulin-Gal80^{ts}*. Transferring the resulting larvae from 18°C to 29°C triggered excision of the ***FRT.NRT-Wg.FRT cassette in patches of cells within the P compartment. No anti-HA immunoreactivity (i.e. NRT-Wingless) could be detected in the patches 12 hours after the temperature shift (red and white arrows in Figure 1i). Since residual Gal80^{ts} activity perdures as late as 5 hours after shifting to 29°C [25], we estimate that NRT-Wingless persists for less than 7 hours and is therefore not unusually stable. Importantly, lack of anti-HA staining within the patches also shows that no detectable Wingless is released from NRT-Wingless-expressing cells. The range of NRT-Wingless was functionally assessed by analysing the expression of *wingless* target genes *(senseless* and *distalless*) in *wingless* null mutant clones generated in a *wg[KO; NRT-Wg]* background ('null-in-NRT'). For comparison, *wingless* null mutant clones were also induced in a wild type background ('null-in-wt'). In both cases, *senseless* was only activated within one cell diameter from the clone edge (Extended Data Figure 2a, b). Therefore, NRT-Wingless achieves the level of signaling required to activate *senseless* expression. Next we assessed the range of NRT-Wingless with *distalless*, a target gene thought to require lower signaling activity. 'Null-in-NRT' clones located in region 1 (clones located elsewhere will be addressed later) failed to maintain *distalless* expression except in adjoining cells (red arrows in Fig. 2b). By contrast, *distalless* expression was maintained throughout similarly sized and positioned 'null-in-wt' clones (turquoise arrowhead in Fig. 2a). These results confirm that wild type Wingless can spreads over a few cell diameters [4] and that, in region 1, Wingless signaling is continuously required for high *distalless* expression. Importantly they also demonstrate that no active Wingless or other functional Wnts is released from the NRT-Wingless expressing cells.

Prolonged transcriptional activity and cellular memory

So far we have shown that NRT-Wingless does not act beyond adjoining cells and yet, extensive genetic analysis has shown that Wingless signaling is required within the prospective wing blade, seemingly far from the source of Wingless [4,5,21,26]. The combined effect of two processes provides a solution to this paradox. One such process was revealed by careful analysis of the pattern of *wingless* transcription. This was facilitated by inserting a Gal4-encoding cDNA into the *attP* site of the *wg[KO]* allele, and crossing the resulting flies *(wg[KO; Gal4])* to flies carrying UAS-GFP (Fig. 3a). GFP signal could be seen throughout the pouch until mid-3rd instar stage, suggesting that 'the Wingless target cells' are indeed transcribing *wingless* during this period of development. Since the perdurance of GFP could lead to an overestimate of the time when transcription terminates, we devised a Flp-gated reporter of *wingless* transcription, comprising *wg[KO; **FRT**.Wg.**FRT** QF], hs-Flp and QUAS-Tomato* (Fig. 3b). Heat shocks at early 3rd instar led to the induction of Tomato-expressing clones throughout the prospective wing, while the clones induced later became spatially restricted. A similar behaviour was seen with another reporter designed to provide a permanent record of transcriptional activity at experimentally defined times (Extended Data Figure 3b, c). To confirm directly that *wingless* is transcriptionally active, imaginal discs where processed for fluorescence *in situ* hybridization (FISH) with a *wingless* probe. Specific signal (using the prospective notum as a negative control) was

seen in the prospective wing region as late as 84±3 hours after egg laying (Fig. 3c; see also [13]). Therefore multiple experimental approaches showed that *wingless* transcription is active throughout the wing pouch during a critical period of patterning and growth (see also [14]), but then recedes towards the D-V boundary during the first half of 3rd instar. Imaginal discs of larvae carrying *wg[KO; Gal4]* and *UAS-HRP-CD8-GFP*, a particularly stable reporter [27] vividly illustrate that all the cells of the prospective wing blade derive from cells that express *wingless* during early third instar (Fig. 3d). The *wingless* transcriptional program could provide a local source of low level protein in the prospective wing blade during the first part of 3rd instar.

Although *wingless* transcription in the prospective blade extends later than previously thought, it does terminate around the mid-3rd instar. Therefore an additional mechanism is needed to sustain growth and patterning without releasable Wingless beyond this stage. The nature of this mechanism is suggested from the behaviour of *vestigial* and *distalless* in response to changes in Wingless signaling. As expected from classical target genes, these two genes are activated by ectopic signaling activity and their expression terminates in small patches of cells that are made unable to respond to Wingless (e.g. by genetic removal of the receptors) [4,5,22]. However, unlike classical target genes, their expression persists, albeit at a reduced level, when signaling is prematurely terminated throughout the disk or a compartment [21,26]. Such persistence can be seen for *distalless* in regions 2 and 3 of 'null-in-NRT' mosaic discs. For example, in clones that transect the D-V boundary in the central portion of the disc (region 2), *distalless* expression was reduced but not eliminated (e.g pink arrowhead in Fig. 2c). Note that high *distalless* continued to be expressed in null-in-NRT cells located at the edge of the clones, both in region 1 and in region 2 (red arrows in Fig. 2b and 2c). By contrast, high *distalless* expression was maintained throughout similarly sized null-in-wt clones (Fig 2a). These observations further confirm that the NRT territory only triggers juxtacrine signaling. In region 3, further away from the D-V boundary, *distalless* expression was essentially unchanged in 'null-in-NRT' clones (yellow asterisk in Fig. 2c), again confirming that *distalless* expression persists in this region even after removal of Wingless signaling. Persistent target gene expression within 'null-in-NRT' clones could explain their continued albeit slower (in comparison with null-in-WT) growth (Extended Data Figure 2c-f). Memory of earlier signaling, which has been suggested previously for Dpp [28], could involve classical epigenetic control. Indeed, the expression of a *vestigial* reporter construct has been shown to be influenced by the presence or absence of Polycomb response elements [29]. Autoregulation could also contribute to the sustained expression of target genes [30]. Irrespective of the underlying mechanism, persistence of target gene expression could explain, in part, why *wg[KO; NRT-Wg]* discs continue to grow beyond the time when *wingless* transcription terminates in the prospective wing blade. It also suggests that during normal development, target gene expression within the prospective blade (region 3) does not necessarily require Wingless to spread from the D-V boundary.

Organ growth and developmental timing

Even though *wg[KO; NRT-Wg]* homozygous flies are morphologically normal, larvae of this genotype entered pupariation with a delay compared to controls (Fig. 4a). In addition, although they eclosed at a near normal frequency when cultured on their own, they largely

failed to do so in co-culture with controls (Fig. 4b); a strong indication of reduced fitness. Since imaginal disc damage can delay larval development[31–33], it is conceivable that preventing Wingless release could affect developmental timing of the larva indirectly by slowing down disc development. To test this possibility, we developed a method for tissue-specific allele switching in second instar imaginal discs [24] (Extended Data Figure 4a, b). Thus, we created larvae expressing wild type Wingless throughout except in imaginal discs, where NRT-Wingless was expressed instead *wg[KO; WT^{Body}; $NRT\text{-}Wg^{Discs}$]* (Fig. 4c, d). Larvae of this genotype developed at the same rate as controls (Extended Data Figure 4c) and eclosed at near normal frequency when co-cultured with control siblings (Fig. 4e). By contrast, larvae expressing wild type Wingless in imaginal discs and NRT-Wingless elsewhere *wg[KO; $NRT\text{-}Wg^{Body}$; WT^{Discs}]* (Fig. 4j, k) largely failed to eclose when co-cultured with control siblings even though they grew into normal-looking adults when grown in separate vials (Fig. 4l, n, p). These observations suggest that Wingless release, or signaling activity not achieved by NRT-Wingless, is required in tissues other than imaginal discs for timely development and general fitness. Nevertheless, further analysis of *wg[KO; WT^{Body}; $NRT\text{-}Wg^{Discs}$]* flies suggested that, in addition, the growth rate of imaginal discs expressing *NRT-Wg* is autonomously compromised. The wings of such mosaic flies were smaller than those of controls (-23%, Fig. 4f-h and Extended Data Figure 4d). This constitutes a more extreme size reduction than that seen in wings obtained from animals expressing NRT-Wingless throughout *(wg[KO; NRT-Wg];* -12%). One likely interpretation is that, in the absence of Wingless release, imaginal disc growth slows down in an organ-autonomous manner, preventing a normal size to be reached in larvae that develop at a normal rate, as in the case in the *wg[KO; WT^{Body}; $NRT\text{-}Wg^{Discs}$]* genotype. To confirm this possibility, we measured disc size in *wg[KO; WT^{Body}; $NRT\text{-}Wg^{Discs}$]*, *wg[KO; NRT-Wg]*, and control animals at the onset of pupariation. The results showed that Wingless tethering specifically in imaginal discs causes a ~15% size deficit (Extended Data Figure 4e-g), a relatively mild reduction considering that growth occurs over a period of about 4 days. Another noteworthy feature of *wg[KO; WT^{Body}; $NRT\text{-}Wg^{Discs}$]* flies is that their wing margin lacked occasional sensory bristles (Fig. 4i), a phenotype not seen in homozygous *wg[KO; NRT-Wg]* flies grown in optimal conditions (Extended Data Figure 1m-o). Since margin specification occurs at the very end of larval life, we suggest that, in *wg[KO; WT^{Body} ; $NRT\text{-}Wg^{Discs}$]* flies, the margin cannot be completed for lack of time before pupariation (see Methods for another example of wing-body asynchrony). The above considerations suggest that a disc-autonomous growth delay does not hold up the developmental progression of the organism and therefore that, at least in this instance, there is no organ size control checkpoint. Moreover, our mosaic analysis by allele switching also shows that Wingless release, or a level of signaling activity not achieved by NRT-Wingless (see Methods for further discussion on their relative importance), contributes independently to ensuring timely growth in an organ-specific manner and to pacing organismal developmental progress.

Conclusion

In this paper we have asked directly to what extent the spread of Wingless, the main Wnt of *Drosophila*, is required for normal development of the wing. Transcription of *wingless* takes

place throughout wing precursors at early stages, and later becomes restricted to a narrow stripe at the D-V boundary. From there, the protein product spreads to form a gradient [4,5,34], as expected from a morphogen. However, the requirement for graded expression has been questioned [21]. In addition, as we showed here, juxtacrine Wingless signaling suffices for extensive growth and patterning. Early *wingless* expression throughout the wing primordium, along with the persistent effect of signaling [21,26,35] ensure continued target gene expression in the absence of Wingless release. We infer that these processes contribute substantially to patterning and growth in the wild type. Nevertheless, target genes remain responsive until late stages [4,5]. Therefore, Wingless spreading from the D-V boundary likely boosts proliferation, at least in cells within its reach. Our results, along with those of previous studies [14,21,35–37], suggest that the requirement for long-range spreading of other Wnts should be revisited. Furthermore our genome editing approach and associated tools for mosaic analysis provide a template for further investigation of other signaling proteins.

Methods

Editing the wingless locus

Gene targeting was performed with a targeting vector and protocol described elsewhere [24]. The primers used to amplify homology arms and to confirm gene targeting are listed below.

Primer	**Sequence, 5’ > 3’**
Forward, 5’ arm	GATCAGTGCGGCCGCGCCGAGAAGAGATCGCCACCACCACTCTACTCTTTTGCACATGCC
Reverse, 5’ arm	GATCGCTAGCCGGCACACACACTCTCACACTGACACACGGGGTATGATAGATACTTCC
Forward, 3’ arm	GATCATGCATGGACACTGCCCGCCTCCAGCCCAGTCCCGTCCTCTGAAGCCGCCC
Reverse, 3’ arm	GATCCCTAGGGCCGATCTGTTGCAATTTCCAAATCAAACAGCGCGCGAAACGTGTGGC
For confirmation of 5’ recombination (genomic, forward)	CAGCACTAAAATGGCTTCCTCCGC
For confirmation of 5’ recombination (vector, reverse)	CAACTGAGAGAACTCAAAGG (within *attP* site)
For confirmation of 3’ recombination (vector, forward)	TCGTATAATGTATGCTATACG (within Gal4 Poly A)
For confirmation of 3’ recombination (genomic, reverse)	GTTCCCGGAATAGTTTAGACCTC

After confirmation of targeting into *wingless*, much of the targeting vector was removed by crossing to a strain expressing Cre constitutively (Bloomington stock 851) (procedure outlined in [24]). The resulting strain, referred to as *wg[KO]* in the manuscript was used as a

host for reintegration of various constructs via the *attP* site. Reintegration was achieved by injecting a *wg[KO]* strain expressing the PhiC31 integrase.

The following constructs were reintegrated:

* **RIV$^{Wg/White}$** (Extended Data Figure 1d): The full length *wingless* cDNA, along with 135 bp of 5'UTR and 1200 bp of 3'UTR was inserted as a NotI-AscI fragment into **RIV** ^{white} [24].
* **RIV$^{FRT,Wg,FRT\ QF}$** (Fig. 3b): This was obtained by cloning the above NotI-AscI *wingless* fragment into **RIV** ^{FRT}.MCS2.$^{FRT\ QF}$, which is described in [24].
* **RIV$^{NRT\text{-}Wg/White}$** (Fig. 1a-c, Extended Data Figure 1e): First, **pMT-NRT-Wg** was made by replacing the NotI-BglII fragment of **pMT-Wg** with a synthetic fragment (GENEWIZ, USA) containing, from 5' to 3', the 5'UTR of *wingless*, the Neurotactin open reading frame, DNA encoding two HA epitopes, and remaining *wingless* coding sequences (up to the BglII). DNA encoding NRT-HA-Wg was then transferred to **RIV^{white}** as a NotI-AscI fragment.
* **RIV$^{FRT,NRT\text{-}HA\text{-}Wg,FRT\ QF}$** (Fig. 1i): This was obtained by cloning the above Notl-AscI NRT-HA-Wingless fragment into **RIV$^{FRT.MCS2.FRT\ QF}$**, which is described in [24].
* **RIV^{Gal4}** (Fig. 3a, Extended Data Figure 3c): This is described elsewhere [24].
* **RIV$^{FRT.Wg.FRT\ NRT\text{-}Wg}$** (Fig. 4c, Extended Data Figure 4b): First, the QF open reading frame was excised from **RIV$^{FRT.Wg.FRT\ QF}$** with AvrII and AgeI and replaced by an Xbal-AgeI fragment containing NRT-HA-Wg obtained from **pMT-NRT-HA-Wg**.
* **RIV$^{FRT.NRT\text{-}Wg.FRT\ Wg}$** (Fig. 4j): An XbaI-AgeI fragment encoding Wingless was obtained from **pMT-Wg** and cloned into **RIV$^{FRT.NRT\text{-}Wg.FRT\ QF}$** pre-digested with AvrII and AgeI.

Immunostaining, FISH and microscopy

The following primary antibodies were used: rabbit anti-HA (1:1000, Cell Signalling Technology, C29F4), mouse anti-Wingless (1:100, Hybridoma Bank), rabbit anti-Vestigial (1:50, gift from S. Carroll), mouse anti-Distalless (1:300, gift from S. Carroll), Rabbit anti-Senseless (1:500, gift from H. Bellen), and chicken anti-β–galactosidase (1/200, Abcam). Secondary antibodies labelled with Alexa 488 or Alexa 555 (used at 1:200) were obtained from Molecular Probes. Imaginal discs were mounted in Vectashield with DAPI (Vector Laboratories). In all micrographs, blue staining shows DAPI, a nuclear marker. Staining for HRP activity with DAB was performed as previously described [27]. Fluorescence *in situ* hybridisation was performed according to standard protocols [38]. Fluorescence micrographs were acquired with a Leica SP5 confocal microscope. Embryo cuticles were prepared according to standard protocol. Bright field images from embryo cuticles were obtained with a Zeiss Axiophot2 microscope with an Axiocam HRC camera. Bright field and confocal images were processed with Photoshop CS4 (Adobe). Measurement of adult wing size,

cell density and generation of fluorescence intensity profiles in wing imaginal discs are described previously [21].

Temperature shifts to assess NRT-Wingless perdurance and wingless promoter activity

The perdurance of NRT-Wingless was estimated in larvae of the genotype *wg[**FRT**.NRT-ts WgFRT QF]/wg[KO]; hedgehog-Gal4 tubulin-Gal80^{ts}/UAS-Flp* (Fig. 1i). Larvae of this genotype were kept at 18°C until mid-late 3rd instar. They were then transferred to 29°C for 12 hours to allow excision of NRT-Wg. Under these conditions, excision occurred in groups of cells without any apparent spatial reproducibility. To assess the activity of *wingless* promoter, *wg[KO; Gal4], tubulin-Gal80^{ts}/Cyo* flies were crossed to flies carrying *UAS-Flp* (Bloomington stock number 4539) and *Actin-**FRT**.stop.**FRT**-Lac-Z* (Bloomington stock number 6355). The progeny were allowed to lay eggs for 24 hours at 18°C and the resulting larvae were kept at 18°C until shifting to 29°C at different times. Larvae were allowed to continue development at this temperature until late wandering stage, before puparation. The timeline of this protocol is illustrated in Extended Data Figure 3b. In both experiments imaginal discs were then processed for conventional immuno-fluorescence.

Assessing the size of wingless mutant territories

wingless mutant territories were generated with *hedgehog-gal4* and *UAS-flp*, which trigger mitotic recombination in virtually all cells of the P compartment at early stages of larval development. In control experiments [26], genetically marked wild type tissue generated in a wild type background occupied half of the posterior compartment. Unlike standard heat shock-induced clonal analysis, this approach overcomes the issues raised by differences in developmental timing between controls and experimentals. The genotypes used to generate the data shown in Extended Data Figure 2c-f were:

FRT$_{40}$ *wg^{CX4}*/**FRT$_{40}$** Ubiquitin-GFP; *hh-Gal4, UAS-Flp* (Extended Data. Fig. 2c) **FRT$_{40}$** *wg^{CX4}*/**FRT$_{40}$** Ubiquitin-GFP *NRT-Wg; hh-Gal4, UAS-Flp* (Extended Data. Fig.2d) For both genotypes, larvae were dissected and fixed at the end of 3rd instar, before pupariation. At least 30 confocal planes were combined by maximal projection. The areas of GFP-positive and GFP-negative territories were measured in the prospective wing blade (area encircled by white dots in Extended Data Figure 2e) with ImageJ. Over 10 discs were analysed for each genotype.

Normalised eclosion rates

For co-culture assays, eggs deposited by balanced flies were allowed to develop in a single vial and all the eclosed adults were genotyped (using the dominant marker on the balancer chromosome). The number of experimental (non-balancer) was normalised to the mendelian ratio-adjusted number of sibling controls (balancer). For example, eggs deposited by *wg[KO; NRT-Wg]/Cyo* gave rise to homozygous *wg[KO; NRT-Wg]* (experimental) and *wg[KO; NRT-Wg]/Cyo* (control) flies. Since these are expected in a 1:2 ratio, the normalized eclosion rate was calculated as (# experimentals)/(0.5 x # controls). Note that the normalized eclosion rate can be larger then 100% since balancer chromosomes are likely to reduce fitness. For separate culture experiments, first instar larvae (24-28h after egg laying) were genotyped using GFP-expressing balancer chromosomes. Fifteen larvae of each

genotype were then transferred into separate vials and kept at 25° C under normal laboratory conditions. The number of eclosed experimental flies was normalized to the number of eclosed control.

Time of puparation

First instar larvae (24-28h after egg laying) were genotyped using GFP-expressing balancer chromosomes. 10-15 larvae of each genotype were transferred into separate vials and kept at 25° C under normal laboratory conditions until they started puparation. The number of larvae pupariating within 2 hour interval was then recorded. At least four independent experiments were performed for each genotype (Fig. 4a).

Genetic markers of reintegration

Depending on experimental requirements, two genetic markers, *mini-white* and *pax*-Cherry, were used alternately to track reintegrated genetic elements (as shown for *wg[KO; NRT-Wg]* in Extended Data figure 1e). We found that the presence of *miniwhite* and *pax-Cherry* downstream of the reintegrated cDNA had an equally detrimental impact on quantifiable physiological functions such as developmental progression (see below), and organismal motility (not shown). Although the choice of marker is unlikely to be relevant, marker usage is listed below for each figure.

Fig. 1a: *wg[KO; NRT-Wg*, pax-Cherry*]*

Fig. 1b, Fig. 1d (anti-Distalless): *wg[KO; NRT-Wg*, mini-white*]*

Fig. 1d (Fz3-GFP): *wg[KO; NRT-Wg*, pax-Cherry*]/wg[KO; NRT-Wg*, mini-white*]*

Fig. 1h: *wg[KO; NRT-Wg;* pax-Cherry*]*

Fig. 1i: *wg[KO;**FRT**.NRT-Wg.**FRT** QF;* pax-Cherry*]*

Fig. 2: *wg[KO; NRT-Wg*, mini-white*]*

Fig. 3a: *wg[KO; Gal4*, mini-white*]*

Fig. 3b: *wg[KO;**FRT**.NRT-Wg.**FRT** QF;* pax-Cherry*]*

Fig. 4a-e and g-i: *wg[KO;**FRT**. Wg.**FRT** NRT-Wg;* pax-Cherry*]*

Fig. 4j-l and n-p: *wg[KO;**FRT**.NRT-Wg.**FRT** Wg;* pax-Cherry*]*

Extended Data Figure 1f-o: *wg[KO; Wg*, mini-white*] or wg[KO; NRT-Wg*, mini-white*]*Extended Data Figure 2b, d, f: *wg[KO; NRT-Wg*, mini-white*]*

Extended Data Figure 3c: *wg[KO; Gal4*, mini-white*]*

Extended Data Figure 4b-g: *wg[KO;**FRT**.Wg.**FRT** NRT-Wg;* pax-Cherry*]* or *wg[KO;**FRT**.NRT-Wg.**FRT** Wg;* pax-Cherry*]*

Europe PMC Funders Author Manuscripts

Removal of the genetic marker from wg[KO; NRT-Wg] preferentially ameliorates developmental timing

In preliminary experiments, we assessed the phenotypic effect of removing, by Cre-mediated excision, the genetic markers (pax-Cherry or mini-white) of *wg[KO; NRT-Wg]* (see position of the LoxP sites in Extended Data Figure 1e). We found that homozygous *wg[KO; NRT-Wg]*^{Floxed} larvae grew faster and competed more effectively in co-culture than homozygous *wg[KO; NRT-Wg]* larvae (which carried either mini-white or pax-Cherry), a phenotypic improvement that is likely due to enhanced NRT-Wg expression. Yet, the wing margin of homozygous *wg[KO; NRT-Wg]*^{Floxed} flies were seen occasionally to miss sensory bristles in the posterior compartment. This confirms our suggestion that a minor extension of the growth period helps NRT-Wingless flies to make a perfectly patterned wing margin. Our evidence so far is consistent with the notion that the developmental delay of *wg[KO; NRT-Wg]* animals could be due mostly to a mild reduction in expression and hence activity. It remains to be determined whether the wing autonomous growth defect is due to the lack of Wingless release or reduced expression.

Europe PMC Funders Author Manuscripts

Extended Data

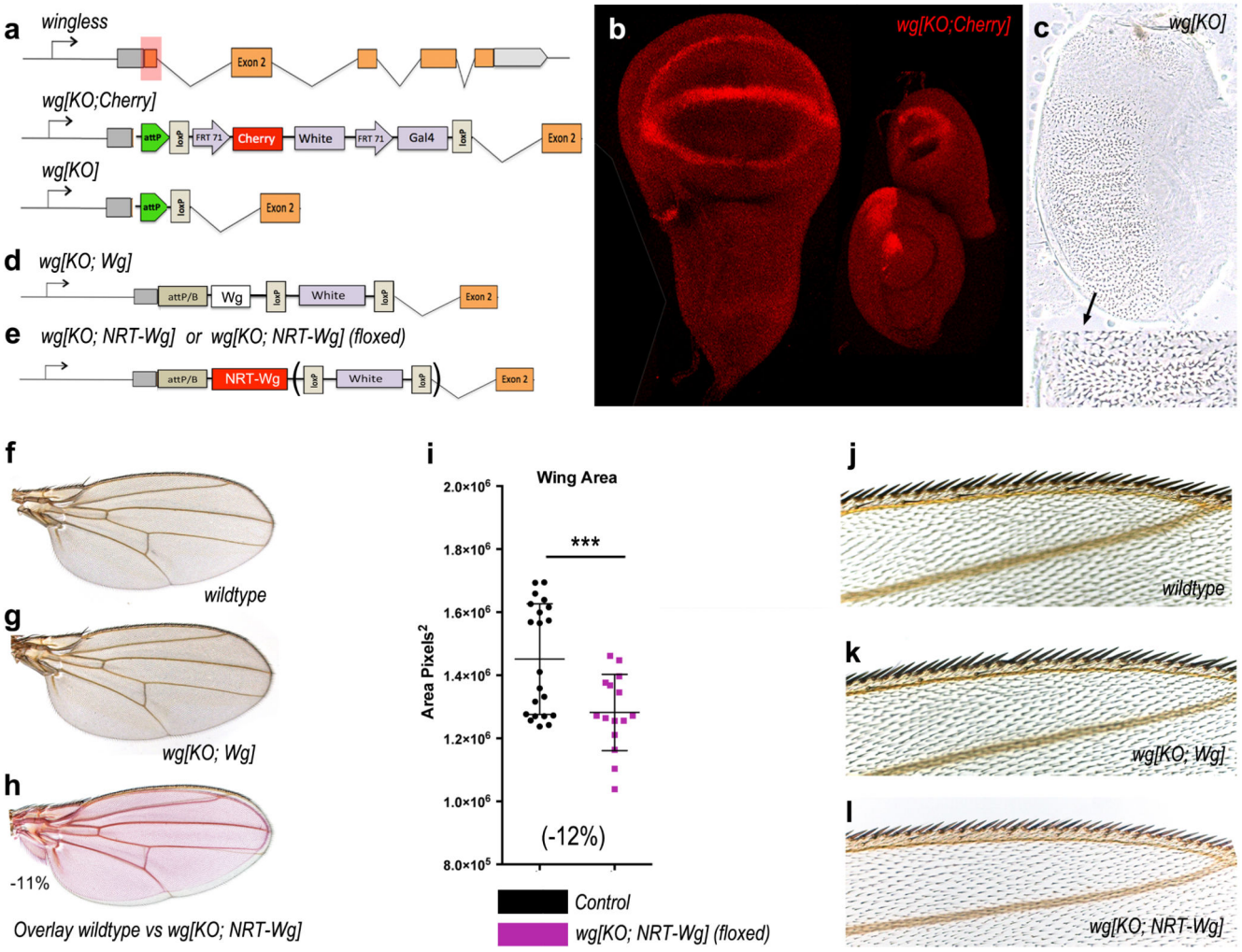

Extended Data Figure 1. Engineering the *wingless* locus to express membrane-tethered Wingless

a, Structure of the *wingless* locus before targeting, after targeting, and after Cre-mediated excision. The *wg[KO]* allele was used as a founder line for subsequent reintegration. **b**, Cherry expression in wing, leg and haltere imaginal discs of larvae carrying one copy of *wg[KO; Cherry]*. **c**, Cuticle preparation of a homozygous *wg[KO]* larva at low and high magnification (black arrow). The phenotype is identical to that of wg^{CX4} homozygous embryos[39]. **d**, Diagram showing the reintegration of a wild type *wingless* cDNA in the *wg[KO]* to generate *wg[KO; Wg]* (note presence of mini-white). **e**, Diagram showing the reintegration of the NRT-Wingless cDNA in *wg[KO]*. This was achieved using either pax-Cherry or mini-white as a genetic marker, as indicated. **f**, Wing of a wild type fly. **g**, Wing of a *wg[KO; Wg]* homozygous fly. **h**, Overlay of the wings shown in Fig. 1b to illustrate the mild wing size reduction in *NRT-Wg* flies. **i**, Wing size of *wg[KO;NRT-Wg]* homozygous (n=14) and control *(wg[KO; NRT-Wg]/GlaBC)* flies (n=16, *** p<0.001). **j-l**, High magnification view of the wing margin of wild type (wild type), homozygous *wg[KO; Wg]*, and homozygous *wg[KO; NRT-Wg]*. They are barely distinguishable. **m-o,**

Views of the dorsal thorax illustrate the normal arrangement of pattern elements such as microchaetes and macrochaetes in the genotypes indicated. Error bars represent standard deviation. Statistical significance was assessed by Student's t-test.

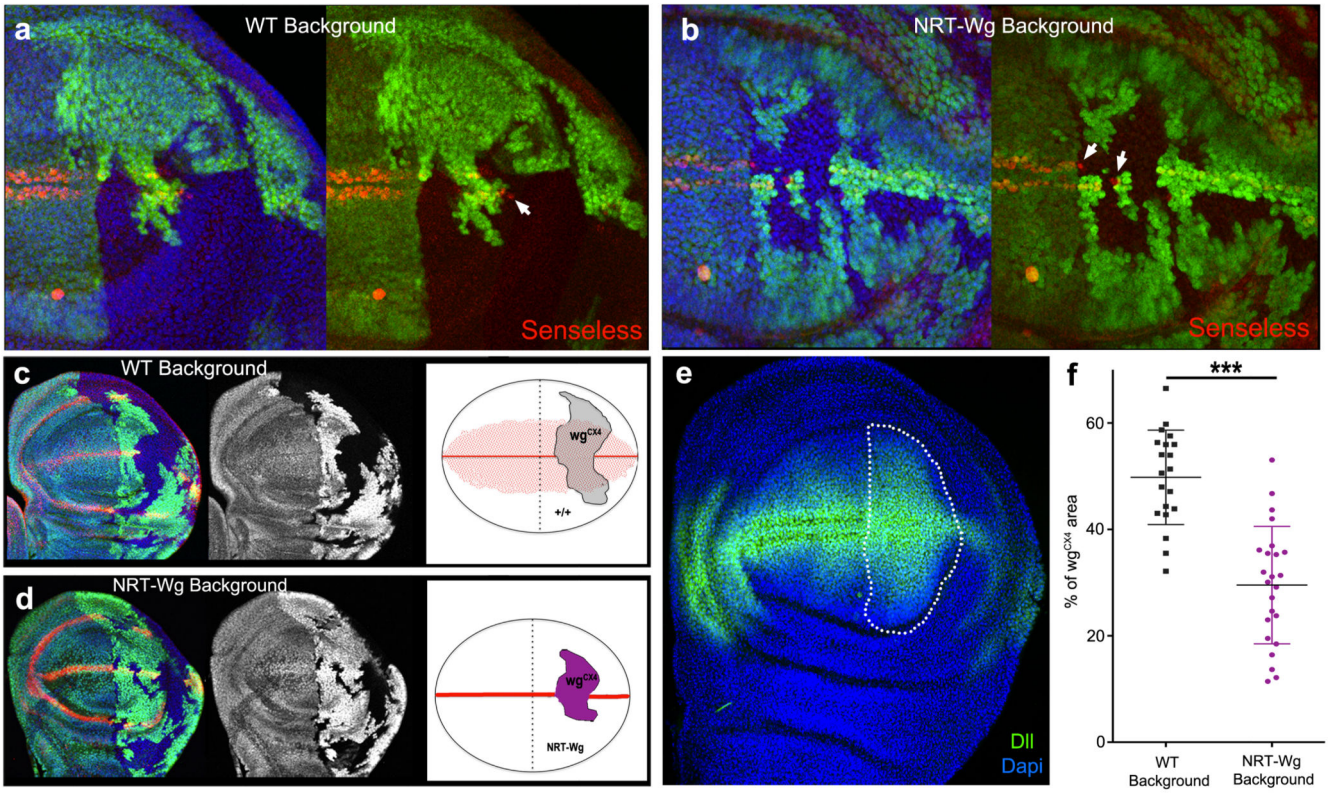

Extended Data Figure 2. Senseless expression and growth in *wingless* null patches surrounded by wild type or NRT-Wingless-expressing cells.

a, **b**, Expression of Senseless (red) is lost in patches of *wingless* mutant cells (GFP-negative; wg^{CX4} homozygotes) except in the cells located within one cell diameter of surrounding GFP-positive cells, which are wild type cells in (a) or homozygous *wg[KO; NRT-Wg]* in (b) (white arrows). Mosaics were created by mitotic recombination in a way that generates approximately the same number progenitors for the two genotypes, as described in Methods. **c**, Example of mosaic imaginal discs generated as above to measure the growth of *wingless* mutant territory *(*wg^{CX4} homozygous; GFP-negative) relative to that of wild type (c) or *wg[KO; NRT-Wg]* homozygous (d) tissue. Wingless and NRT-Wingless, detected with anti-Wingless, are shown in red. **e**, Outline of the territory where the surface areas were assessed. **f**, Quantification of the areas colonised by *wingless* mutant cells (GFP-negative) in the two genetic backgrounds. On average, the *wingless* null territory was smaller in the *wg[KO; NRT-Wg]* homozygous background (n=24) than in the wild type (n=20, *** = p <0.001). Error bars represent standard deviation. Statistical significance was assessed by Student's t-test.

Europe PMC Funders Author Manuscripts

Europe PMC Funders Author Manuscripts

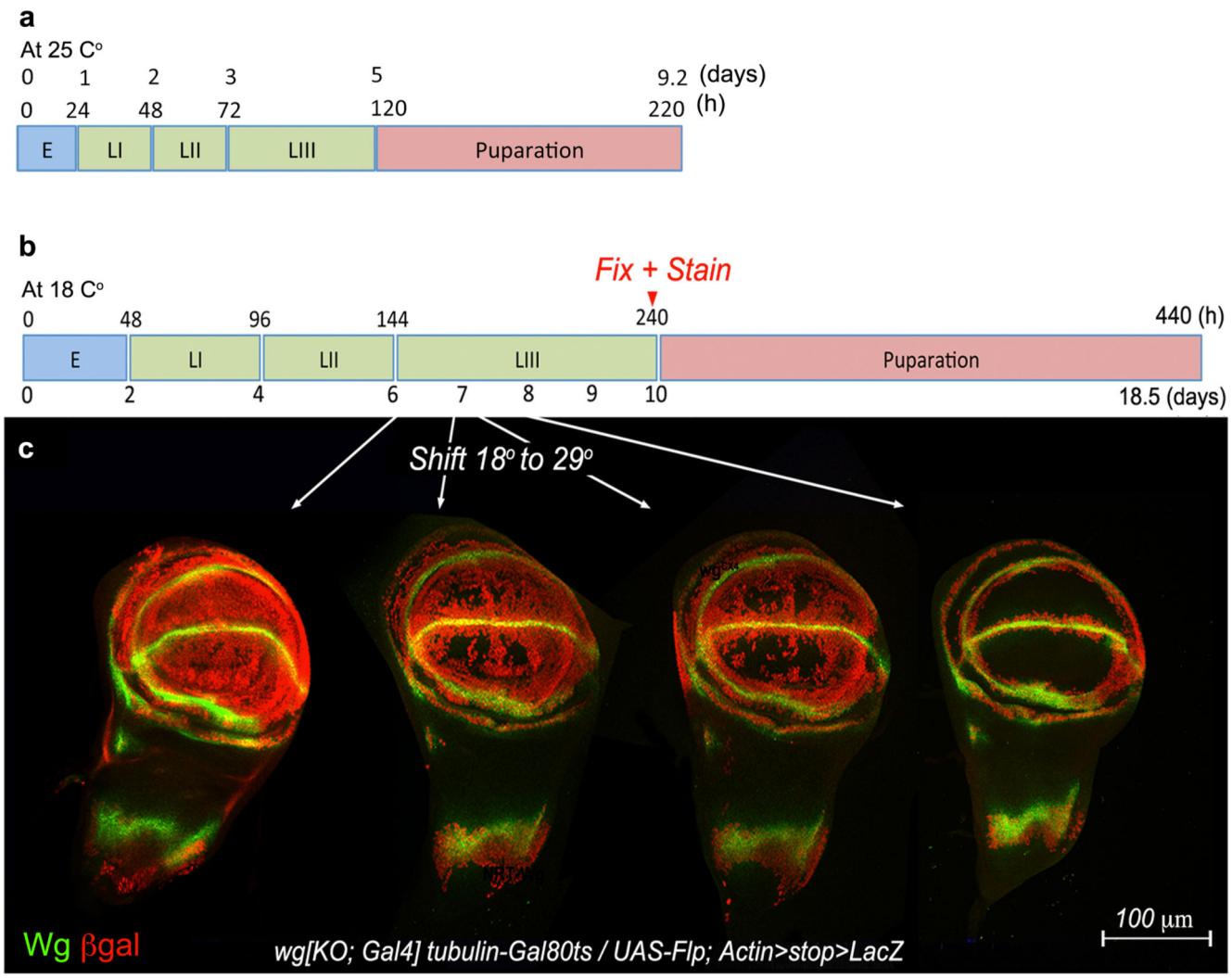

Extended Data Figure 3. Activity of the *wingless* promoter during imaginal disc development.

a, Timing of key developmental stages at 25°C. **b**, Developmental timing at 18°C as it relates to the results illustrated in (c). **c**, Permanent labelling of *wingless*-expressing cells and their descendants at different stages of development. Genotype was *wg[KO; Gal4], tubulin-Gal80^{ts}/UAS-Flp; Actin-**FRT**.stop.**FRT**-Lac-Z* so that the stop cassette was only excised in cells that express *wingless* at the time of shifting to 29°C to activate Flp expression and hence excision of the stop cassette. Discs were shifted from 18°C to 29°C at different stages (shown in b) but they were fixed and stained at the same stage, just before puparation.

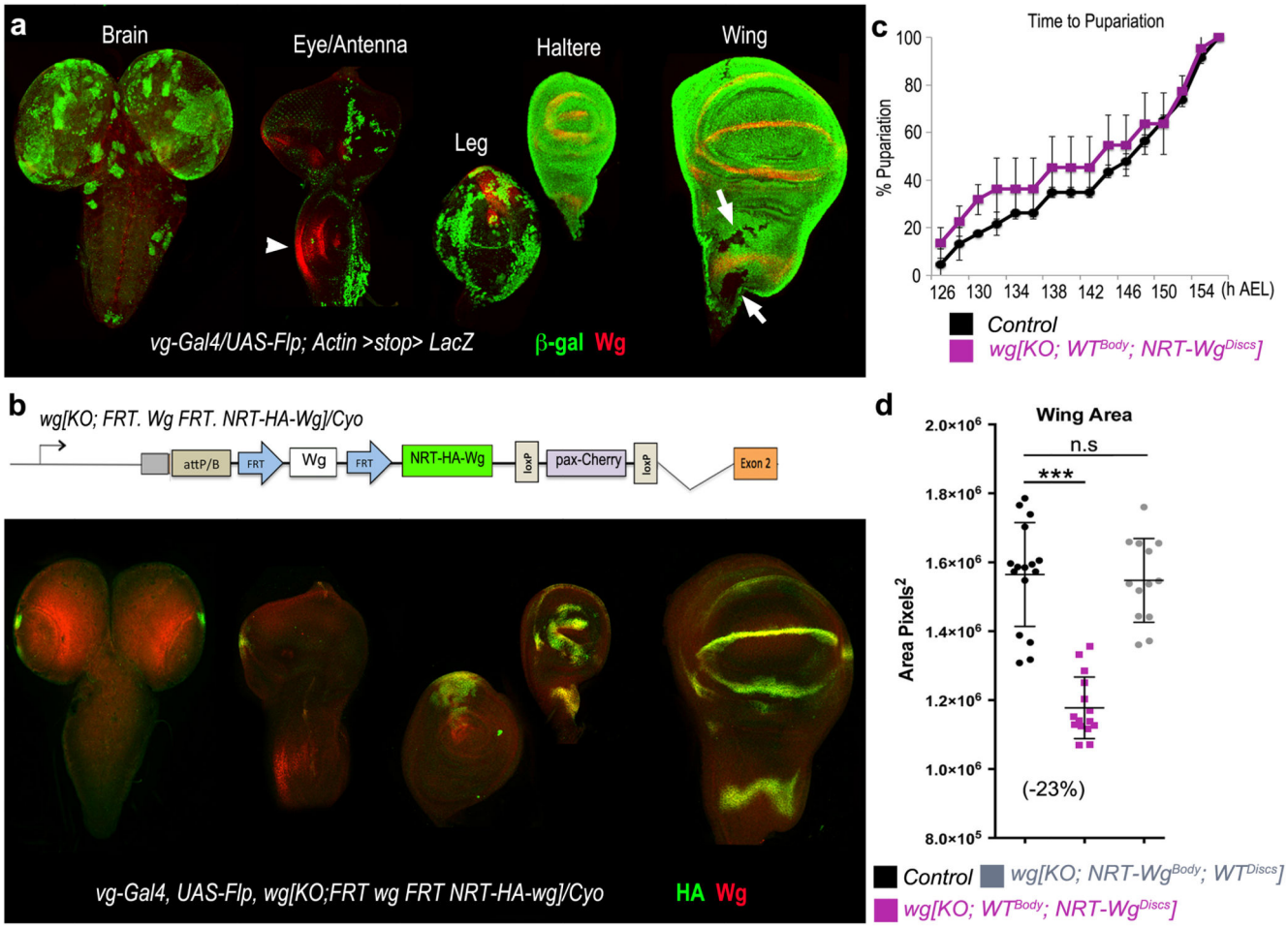

Extended Data Figure 4. Tissue-specific allele switching to determine the anatomical origin of organismal developmental delay in NRT-Wingless animals.

a, Cumulative pattern of *vestigial-Gal4* activity in various organs precursors. Expression of *vestigial-gal4* at any stage or place leads to excision of the stop cassette in *Actin-**FRT**.stop.**FRT**-Lac-Z* thus marking permanently the corresponding cells. As expected, nearly the whole wing and haltere discs were labelled at the end of larval development. In wing imaginal discs, only a few cells were β–Galactosidase-negative that did not overlap with the domain of Wingless expression (anti-Wg, red). In the eye antennal disc, the patterns of Wingless (white arrowhead) and β–Galactosidase expression are also nonoverlapping. Therefore, in combination with *UAS-Flp, vestigial-gal4* is expected to excise an FRT cassette throughout the domain of wingless expression. Examination of the brain and CNS shows that *vestigial-Gal4* is unexpectedly active in these tissues. **b**, In larvae of genotype *vestigial-Gal4, UAS-Flp, wg[**FRT**.Wg.**FRT** NRT-Wg]/Cyo*, most of the *wingless*-expressing cells in leg, haltere and wing imaginal discs, but not in the brain and CNS, were converted to expressing NRT wingless (anti-HA; green). **c**, Developmental timing in *wg[KO; WT^{Body}; NRT-Wg^{Discs}] (vestigial-Gal4, UAS-Flp, wg[**FRT**.Wg.**FRT** NRT-Wg])* and control *(vestigial-Gal4, UAS-Flp, wg[**FRT**.Wg.**FRT** NRT-Wg]/GlaBC)* larvae (80 animals, 4 experiments). The two data sets cannot be statistically distinguished (p>0.05).

Europe PMC Funders Author Manuscripts

d, Adult wing size for three genotypes: 1) In black, *wg[KO; WT^{Body}; NRT-Wg^{Discs}/GlaBc* obtained from selfed *vestigial-Gal4, UAS-Flp, wg[**FRT**.Wg.**FRT** NRT-Wg]/GlaBc)* (n=16), 2) in purple, *wg[KO; WT^{Body}; NRT-Wg^{Discs}]*, obtained from homozygous *vestigial-Gal4, UAS-Flp, wg[**FRT**.Wg.**FRT** NRT-Wg])* (n=15), and 3) in grey, *wg[KO; NRT-Wg^{Body}; WT^{Discs}]*, obtained from homozygous *vestigial-Gal4, UAS-Flp, wg[**FRT**. NRT-Wg.**FRT** Wg])* (n=13). **e-g,** Extent of *distalless* expression in *wg[KO; WT^{Body}; NRT-Wg^{Discs}]* heterozygotes (over Cyo; e) and homozygotes (f). All the discs were obtained from immobile larvae at the time of anterior spiracle eversion, an event that marks the onset of pupariation. The extent of the *distalless* domain was estimated from the surface area of a polygon drawn around the zone of immunoreactivity, as shown. The results, plotted in panel g, show a mild reduction in *wg[KO; WT^{Body}; NRT-Wg^{Discs}]* discs (n=13) compared to controls (n=20; *** = $p<0.001$; n.s. = not significantly different). Error bars represent standard deviation. Statistical significance was assessed by Student's t-test.

Supplementary Material

Refer to Web version on PubMed Central for supplementary material.

Acknowledgements

This work was supported by the UK's Medical Research Council (U117584268), an ERC grant (WNTEXPORT) from the European Union to JPV and a Sir Henry Wellcome post-doctoral fellowship to LAB (082694/Z/07/Z). We are grateful to Ulla-Maj Fiuza for discussion and Alice Mitchell for help in generating the first *wingless* KO allele. Arguments with Gary Struhl have led to significant improvement of the manuscript. We thank colleagues listed in 'Methods Summary', as well as the Developmental Studies Hybridoma Bank and the Bloomington Stock Center for providing antibodies and fly strains.

References

1. van Amerongen R, Nusse R. Towards an integrated view of Wnt signaling in development. Development (Cambridge, England). 2009; 136 :3205–3214. DOI: 10.1242/dev.033910
2. Clevers H, Nusse R. Wnt/β-Catenin Signaling and Disease. Cell. 2012; 149 :1192–1205. DOI: 10.1016/j.cell.2012.05.012 [PubMed: 22682243]
3. Kiecker C, Niehrs C. A morphogen gradient of Wnt/beta-catenin signalling regulates anteroposterior neural patterning in Xenopus. Development (Cambridge, England). 2001; 128 :4189–4201.
4. Zecca M, Basler K, Struhl G. Direct and long-range action of a wingless morphogen gradient. Cell. 1996; 87 :833–844. [PubMed: 8945511]
5. Neumann CJ, Cohen SM. Long-range action of Wingless organizes the dorsal-ventral axis of the Drosophila wing. Development (Cambridge, England). 1997; 124 :871–880.
6. Swarup S, Verheyen EM. Wnt/Wingless signaling in Drosophila. Cold Spring Harbor perspectives in biology. 2012; 4 doi: 10.1101/cshperspect.a007930
7. Garcia-Bellido A, Merriam JR. Parameters of the wing imaginal disc development of Drosophila melanogaster. Dev Biol. 1971; 24 :61–87. [PubMed: 5001010]
8. Johnston LA, Gallant P. Control of growth and organ size in Drosophila. BioEssays : news and reviews in molecular, Cellular and developmental biology. 2002; 24 :54–64. DOI: 10.1002/bies.10021
9. Martín FA, Herrera SC, Morata G. Cell competition, growth and size control in the Drosophila wing imaginal disc. Development (Cambridge, England). 2009; 136 :3747–3756. DOI: 10.1242/dev.038406
10. Williams JA, Paddock SW, Carroll SB. Pattern formation in a secondary field: a hierarchy of regulatory genes subdivides the developing Drosophila wing disc into discrete subregions. Development (Cambridge, England). 1993; 117 :571–584.

11. Couso JP, Knust E, Martinez Arias A. Serrate and wingless cooperate to induce vestigial gene expression and wing formation in Drosophila. Current biology : CB. 1995; 5 :1437–1448. [PubMed: 8749396]
12. Ng M, Diaz-Benjumea FJ, Vincent JP, Wu J, Cohen SM. Specification of the wing by localized expression of wingless protein. Nature. 1996; 381 :316–318. DOI: 10.1038/381316a0 [PubMed: 8692268]
13. García-García MJ, Ramain P, Simpson P, Modolell J. Different contributions of pannier and wingless to the patterning of the dorsal mesothorax of Drosophila. Development (Cambridge, England). 1999; 126 :3523–3532.
14. Martinez Arias A. Wnts as morphogens? The view from the wing of Drosophila. Nature reviewsMolecular Cell biology. 2003; 4 :321–325. DOI: 10.1038/nrm1078
15. Couso JP, Bishop SA, Martinez Arias A. The wingless signalling pathway and the patterning of the wing margin in Drosophila. Development (Cambridge, England). 1994; 120 :621–636.
16. Nolo R, Abbott LA, Bellen HJ. Senseless, a Zn finger transcription factor, is necessary and sufficient for sensory organ development in Drosophila. Cell. 2000; 102 :349–362. [PubMed: 10975525]
17. Jafar-Nejad H, Tien A-C, Acar M, Bellen HJ. Senseless and Daughterless confer neuronal identity to epithelial cells in the Drosophila wing margin. Development (Cambridge, England). 2006; 133 :1683–1692. DOI: 10.1242/dev.02338
18. Sato A, Kojima T, Ui-Tei K, Miyata Y, Saigo K. Dfrizzled-3 a new Drosophila Wnt receptor, acting as an attenuator of Wingless signaling in wingless hypomorphic mutants. Development (Cambridge, England). 1999; 126 :4421–4430.
19. Sivasankaran R, Calleja M, Morata G, Basler K. The Wingless target gene Dfz3 encodes a new member of the Drosophila Frizzled family. Mechanisms of development. 2000; 91 :427–431. [PubMed: 10704878]
20. Giraldez AJ, Cohen SM. Wingless and Notch signaling provide cell survival cues and control cell proliferation during wing development. Development (Cambridge, England). 2003; 130 :6533–6543. DOI: 10.1242/dev.00904
21. Baena-López LA, Franch-Marro X, Vincent J-P. Wingless promotes proliferative growth in a gradient-independent manner. Science Signaling. 2009; 2 ra60 doi: 10.1126/scisignal.2000360 [PubMed: 19809090]
22. Zecca M, Struhl G. A feed-forward circuit linking wingless, fat-dachsous signaling, and the warts-hippo pathway to Drosophila wing growth. PLoS biology. 2010; 8 e1000386 doi: 10.1371/journal.pbio.1000386 [PubMed: 20532238]
23. Herr P, Basler K. Porcupine-mediated lipidation is required for Wnt recognition by Wls. Developmental biology. 2012; 361 :392–402. DOI: 10.1016/j.ydbio.2011.11.003 [PubMed: 22108505]
24. Baena-López LA, Alexandre C, Mitchell A, Pashakarnis L, Vincent J-P. Accelerated genome engineering in Drosophila without sequence constraints. Development (Cambridge, England). 2013; 140
25. Bergantiños C, Corominas M, Serras F. Cell death-induced regeneration in wing imaginal discs requires JNK signalling. Development (Cambridge, England). 2010; 137 :1169–1179. DOI: 10.1242/dev.045559
26. Piddini E, Vincent J-P. Interpretation of the wingless gradient requires signaling-induced self-inhibition. Cell. 2009; 136 :296–307. DOI: 10.1016/j.cell.2008.11.036 [PubMed: 19167331]
27. Dubois L, Lecourtois M, Alexandre C, Hirst E, Vincent JP. Regulated endocytic routing modulates wingless signaling in Drosophila embryos. Cell. 2001; 105 :613–624. [PubMed: 11389831]
28. Lecuit T, et al. Two distinct mechanisms for long-range patterning by Decapentaplegic in the Drosophila wing. Nature. 1996; 381 :387–393. DOI: 10.1038/381387a0 [PubMed: 8632795]
29. Perez L, et al. Enhancer-PRE communication contributes to the expansion of gene expression domains in proliferating primordia. Development (Cambridge, England). 2011; 138 :3125–3134. DOI: 10.1242/dev.065599

30. Halder G, et al. The Vestigial and Scalloped proteins act together to directly regulate wing-specific gene expression in Drosophila. Genes & Development. 1998; 12 :3900–3909. [PubMed: 9869643]

31. Smith-Bolton RK, Worley MI, Kanda H, Hariharan IK. Regenerative growth in Drosophila imaginal discs is regulated by Wingless and Myc. Developmental cell. 2009; 16 :797–809. DOI: 10.1016/j.devcel.2009.04.015 [PubMed: 19531351]

32. Colombani J, Andersen DS, Láopold P. Secreted peptide Dilp8 coordinates Drosophila tissue growth with developmental timing. Science (New York, NY). 2012; 336 :582–585. DOI: 10.1126/science.1216689

33. Garelli A, Gontijo AM, Miguela V, Caparros E, Dominguez M. Imaginal discs secrete insulin-like peptide 8 to mediate plasticity of growth and maturation. Science (New York, NY). 2012; 336 :579–582. DOI: 10.1126/science.1216735

34. Strigini M, Cohen SM. Wingless gradient formation in the Drosophila wing. Current Biology. 2000; 10 :293–300. [PubMed: 10744972]

35. Giorgianni MW, Mann RS. Establishment of Medial Fates along the Proximodistal Axis of the Drosophila Leg through Direct Activation of dachshund by Distalless. Developmental cell. 2011; 20 :455–468. DOI: 10.1016/j.devcel.2011.03.017 [PubMed: 21497759]

36. Wilder EL, Perrimon N. Dual functions of wingless in the Drosophila leg imaginal disc. Development (Cambridge, England). 1995; 121 :477–488.

37. Couso JP, Bate M, Martínez-Arias A. A wingless-dependent polar coordinate system in Drosophila imaginal discs. Science (New York, NY). 1993; 259 :484–489.

38. Artero R, Furlong EE, Beckett K, Scott MP, Baylies M. Notch and Ras signaling pathway effector genes expressed in fusion competent and founder cells during Drosophila myogenesis. Development (Cambridge, England). 2003; 130 :6257–6272. DOI: 10.1242/dev.00843

39. Alexandre C, Lecourtois M, Vincent J. Wingless and Hedgehog pattern Drosophila denticle belts by regulating the production of short-range signals. Development (Cambridge, England). 1999; 126 :5689–5698.

Europe PMC Funders Author Manuscripts

Europe PMC Funders Author Manuscripts

Methods Summary

All the standard fly strains used in this study are described at http://flybase.org and all experiments were conducted at 25°C unless otherwise indicated. *UAS-HRP-CD8-GFP* encodes a transmembrane protein comprising extracellular HRP, the transmembrane domain of mouse CD8 and intracellular GFP (details upon request). Gene targeting was performed with a new vector and protocol described elsewhere [24]. The key elements of the targeting vector are shown in Extended Data Figure 1a. The homology arms used for targeting of the *wingless* locus were amplified by PCR from a BAC (http://www.pacmanfly.org) with primers listed in Methods. The *mini-white* marker of the targeting vector was used for initial identification of candidate targeted flies. True recombinants were confirmed by several criteria, including expression of Cherry, the phenotype of homozygous animals and PCR (primers and protocols described in Methods). Various constructs were integrated into the *attP* site of the targeted allele with a variety of 'reintegration vectors' [24]. Immunostaining of imaginal discs was performed according to standard protocols with the following primary antibodies: rabbit anti-HA (1:1000, Cell Signalling Technology, C29F4), mouse anti-Wingless (1:100, Hybridoma Bank), rabbit anti-vestigial (1:50, gift from S. Carroll), mouse anti-Distalless (1:300, gift from S. Carroll), Rabbit anti-Senseless (1:500, gift from H. Bellen), and chicken anti-β-galactosidase (1/200, Abcam). In all micrographs, blue staining shows DAPI, a nuclear marker. Fluorescence *in situ* hybridisation was performed according to standard protocols [38]. Temperature shifts were performed by transferring culture vials between incubators maintained at the desired temperatures. Details on measuring developmental timing are provided in Methods. For all quantitative measurements, the error bars represent standard deviation. Samples were normally distributed. Sample size was chosen to ensure statistical significance, which was assessed by Student's t-test using Prism 6.

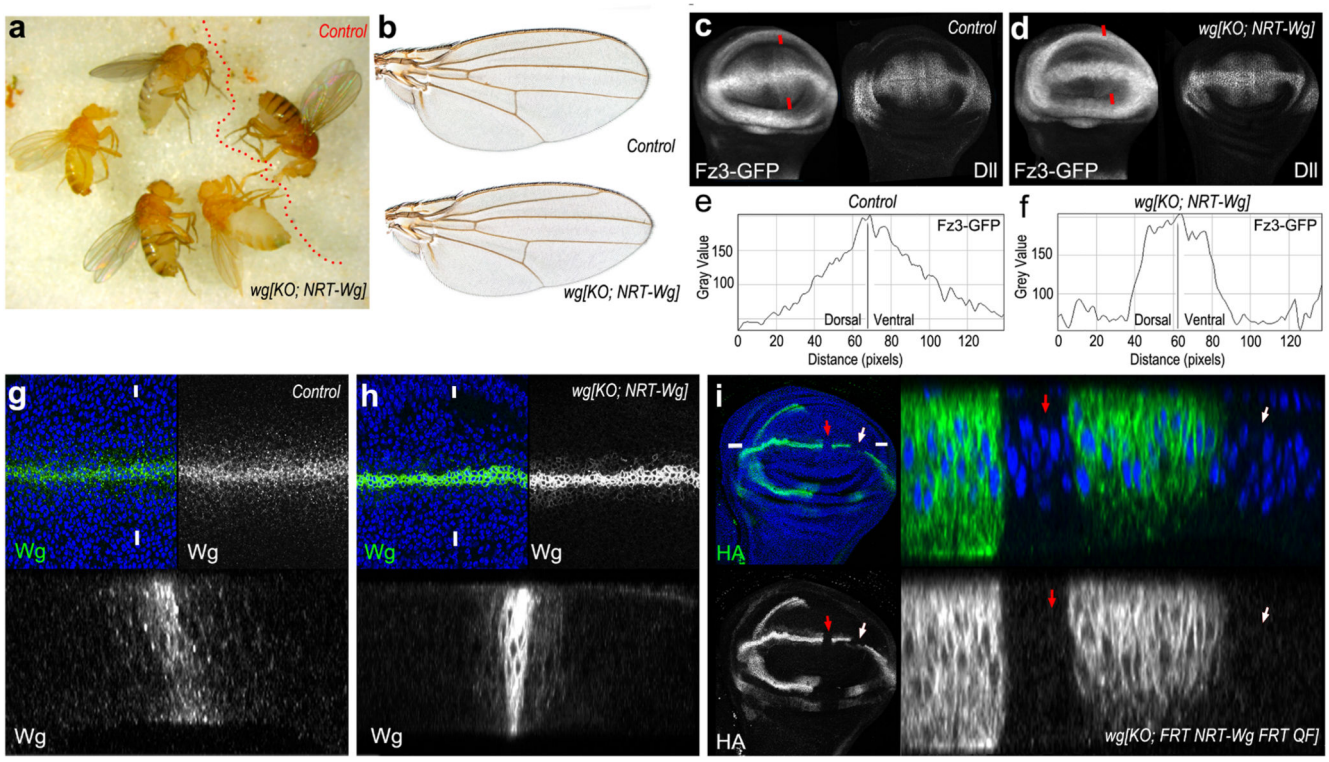

Figure 1. Characterization of membrane-tethered Wingless expressed from the wingless locus

a, Homozygous *wg[KO; NRT-Wg]* flies and one control *(wg[KO; NRT-Wg]/GlaBC)* fly. **b**, Wings from a control *(wg[KO; NRT-Wg]/GlaBC*, and a homozygous *wg[KO; NRT-Wg]* fly (see size information and details of the wing margin in Extended Data Figure 1i-l). **c**, **d**, Expression of Frizzled3-GFP and Distalless in control and homozygous *wg[KO; NRT-Wg]* imaginal discs. **e**, **f**, Fluorescence intensity profile along lines connecting red arrowheads. **g**, **h,** Wingless immunoreactivity in a control (wild type) and a homozygous *wg[KO; NRT-Wg]* disc, with corresponding transverse sections (along line connecting white marks). **i**, Excision of HA-tagged NRT-Wingless (red and white arrows) from *wg[KO; **FRT**.NRT-Wg.**FRT** QF]* with Flp produced from *hedgehog-gal4 tubulin-gal80^{ts} UAS-flp* at 29°C. Low magnification frontal view and high magnification transverse section along line defined by white marks are shown.

Europe PMC Funders Author Manuscripts

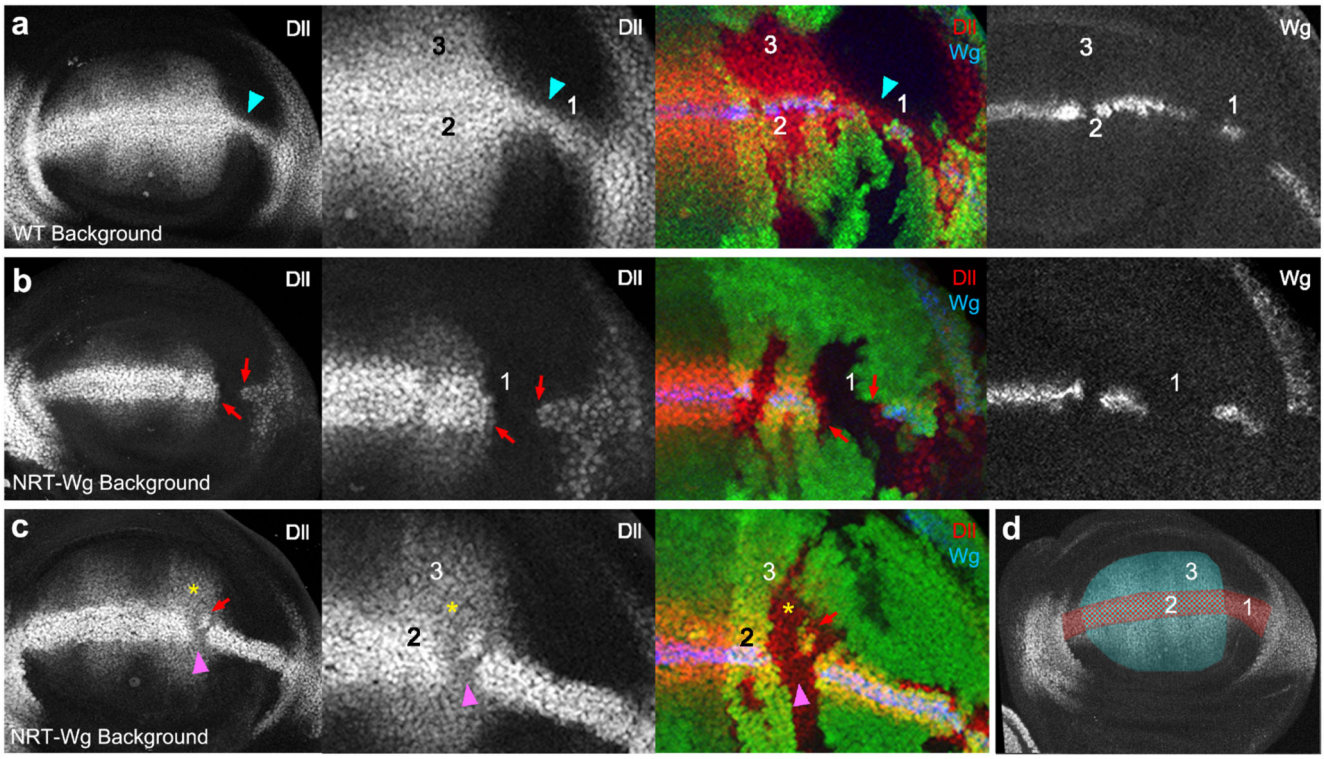

Figure 2. Gene expression in *wingless* null mutant patches surrounded by wild type or NRT-Wingless-expressing cells.

a-c, Expression of Distalless (Dll) and Wingless (Wg), as detected by immunofluorescence, in 'null-in-wt' (a) or 'null-in-NRT' (b, c) clones. Null *wingless* mutant territory *(wg^{CX4})* is marked by the absence of GFP. Red arrows indicate shortrange activation of *distalless* expression by NRT-Wingless. Turquoise arrowhead highlights longer range of wild type Wingless. Pink arrowhead and yellow asterisk indicate persistent expression (memory) in zones 2 and 3 respectively. **d**, Diagram showing regions where the behavior of null mutant clones was analyzed. Region 1 links the prospective wing to the prospective hinge. Region 2 represents the domain straddling the D-V boundary that expresses high level Distalless. Region 3 represents the prospective wing blade, which expresses graded, low level Distalless. Disparities in disc size between panels b and c are due to staging differences.

Europe PMC Funders Author Manuscripts

Europe PMC Funders Author Manuscripts

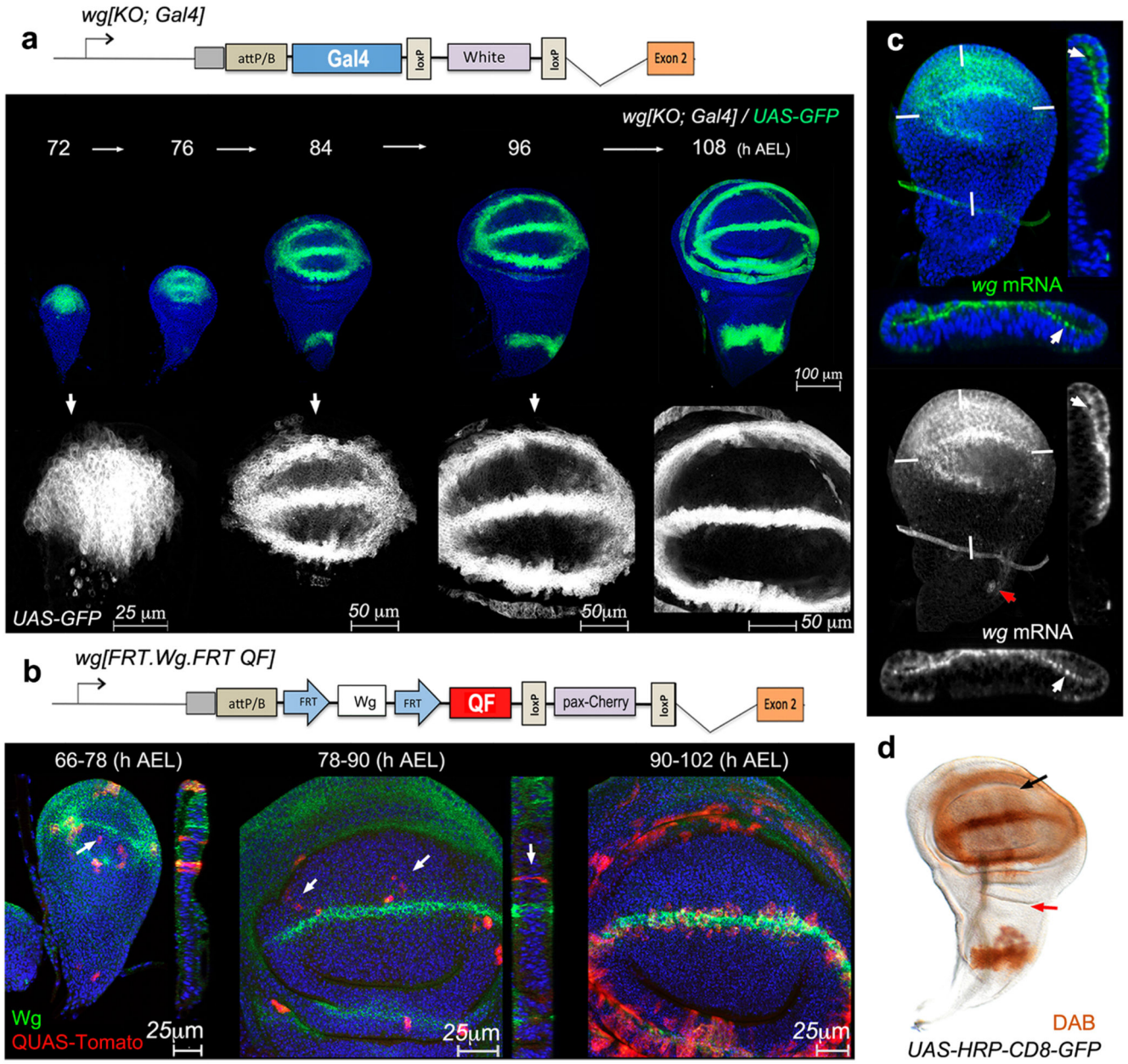

Figure 3. Activity of the *wingless* promoter in the prospective wing.

a, GFP expression driven by *wg[KO;Gal4]* at different stages. **b,** QUAS-Tomato expressing clones in larvae of the genotype *hs-Flp QUAS-Tomato; wg[KO;* ***FRT****.NRT-Wg.****FRT*** *QF]/ Cyo*. Larvae were heat shocked 18 hours before fixation at the times indicated. White arrows indicate the presence of Tomato-expressing cells in the middle of the prospective wing blade, far from the prospective margin. **c**, Fluorescent RNA *in situ* hybridization (FISH) with a *wingless* probe in wing imaginal discs obtained 84±3 hours after egg laying. Red arrow indicates incipient *wingless* expression in prospective thorax. White marks indicate the plane of transverse section. White arrow shows FISH signal in the apical domain. **d**, HRP activity (detected by DAB staining) in a late 3rd instar *wg[KO;Gal4]/+, UAS-HRP-CD8-GFP* wing

imaginal disc. Activity is detectable throughout the pouch (black arrow) but not in the prospective thorax (red arrow).

Europe PMC Funders Author Manuscripts

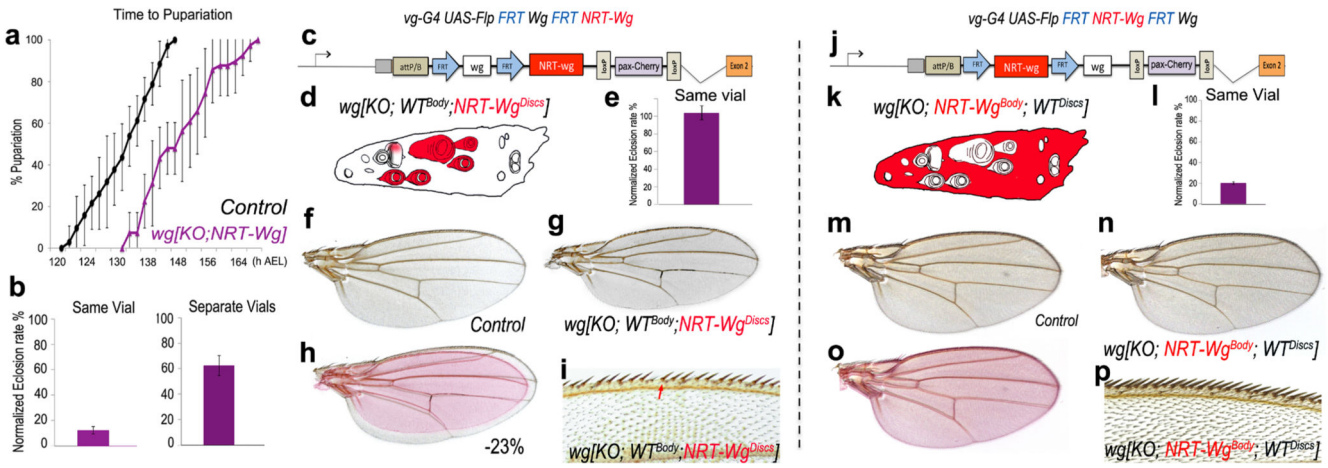

Figure 4. Tissue-specific allele switching to assess the contribution of Wingless release to organ-autonomous growth rate and organismal developmental timing.

a, Homozygous *wg[KO; NRT-Wg]* animals (70 animals, 8 experiments) were developmentally delayed ($p<0.001$) relative to control siblings *(wg[KO; NRT-Wg]/Cyo-GFP;* 34 animals, 6 experiments). Larvae were grown in separate vials. **b**, Normalised eclosion rate of homozygous *wg[KO; NRT-Wg]* larvae cultured with (130 animals, 4 experiments) or without (90 animals, 6 experiments) control siblings. **c, d**, Wingless➔NRT-Wingless conversion with *vestigial-Gal4 UAS-Flp*. Expected NRT-Wingless tissue is shown in red. **e**, Normalised eclosion rate of resulting *wg[KO; WT^{Body}; NRT-Wg^{Discs}]* larvae co-cultured with control siblings (80 animals, 4 experiments). **f-i**, The wings of *wg[KO; WT^{Body}; NRT-Wg^{Discs}]* flies were significantly smaller than those of control siblings (-23%, $p<0.001$) and had an incomplete margin (missing bristles; red arrow). **j, k**, NRT-Wingless➔Wingless conversion with *vestigial-Gal4 UAS-Flp*. **l**, Normalised eclosion rate of the resulting *wg[KO; NRT-Wg^{Body};WT^{Discs}]* larvae co-cultured with control siblings (>140 animals, 4 experiments) was significantly smaller than that of *wg[KO; WT^{Body}; NRT-Wg^{Discs}]* larvae ($p<0.001$). **m**-**p**, The wing size and margin of *wg[KO; NRT-Wg^{Body}; WT^{Discs}]* flies were similar to that of sibling controls ($p>0.05$). Error bars represent standard deviation. Statistical significance was assessed by Student's t-test.